

COUPLING OF LOWER HYBRID WAVES IN THE DOUBLET IIA
HIGH POWER RF HEATING EXPERIMENTS*

by

V. S. Chan, Charles Moeller, and R. W. Gould**
General Atomic Company, San Diego, California 92138

ABSTRACT

In the Doublet IIA high power rf heating experiments, a slow wave is launched by an electrostatic antenna above the lower hybrid frequency. Such an antenna has been proposed previously for generating a well-defined large parallel wavenumber spectrum. In the present experiments, a total of six structures with n_{\parallel} ranging from 11 to 16 at 800 and 915 MHz at power up to 100 kW/structure are being used. The coupling and radiated spectrum are analyzed using the theory developed for these antennas. They are found to be insensitive to changes in plasma parameters.

1. INTRODUCTION

Hitherto, the majority of lower hybrid wave heating experiments have been designed to heat ions through parametric processes or linear mode conversion near the lower hybrid resonance layer.¹ However, it is also possible theoretically that the slow wave branch above the lower hybrid frequency is capable of direct electron heating by Landau damping. Indeed, in a reactor size plasma where the equilibration time is less than the energy confinement time, this offers a viable alternative for bulk heating of tokamak plasmas. In addition, the possibility of current profile control by affecting the local electron temperature presents an attractive approach to stabilizing macroscopic instabilities. The General Atomic lower hybrid heating experiments are designed to explore the feasibility of these ideas.

Unlike experiments that are designed to heat ions, where the only requirement on the parallel wavelength is that accessibility condition be satisfied ($ck_{\parallel}/\omega > 2$), electron heating experiments also require that ω/k_{\parallel} be sufficiently close to the electron thermal velocity. For existing tokamaks ck_{\parallel}/ω as large as 10 or bigger may be necessary. As a result, the evanescent layer which may not be a factor in ion heating experiments becomes significant. In the waveguide "grill" scheme, once ω and k_{\parallel} are chosen, there exist no other variables to compensate for this evanescence. In our experiments, we chose to use a slow wave structure of the more conventional type first analyzed by Golant.²

By placing grounded plates at the point of zero potential between alternately biased radiating elements (Fig. 1), the antenna coupling becomes much less sensitive to changes in plasma conditions. These plates provide an upper limit on the plasma loading of each radiating element to prevent a condition in which the input power would all be radiated by the first few elements. This controlled plasma loading results in a power spectrum which

* Work supported by Department of Energy Contract EY-76-C-03-0167, Project Agreement 38.

** Permanent address: California Institute of Technology

is relatively independent of plasma density gradient. In order to make the most efficient use of the slow wave structure, the impedance of the feedline can be made to increase away from the input to compensate for the plasma loading and thereby maintain the voltage constant along the feedline. A brief description of a quantitative analysis of the structure³ and the numerical results for our parameters are given in the following sections.

2. THEORY

The coupled plasma-antenna system is subdivided into two regions. Inside the antenna, we expand the field bounded by each pair of adjacent plates in a Fourier cosine series in z for $0 \leq x \leq h$:

$$\phi(x, z) = \sum_{p=1}^M \sum_{n=1}^{\infty} \left(a_{np} e^{-k_n x} + b_{np} e^{k_n x} \right) \cos k_n (z - z_p) \Theta_p(z) \quad (1)$$

Here, M is the number of elements in the structure, z_p , the position of the p^{th} element, $z_p = 2(p-1)d$, $k_n = \pi(2n-1)/2d$, and Θ_p is a step function:

$$\Theta_p(z) = \begin{cases} 1 & \text{if } z_p - d \leq z \leq z_p + d \\ 0 & \text{elsewhere} \end{cases}$$

Inside the plasma, the field is represented as a Fourier integral

$$\phi(z, x) = \int_{-\infty}^{\infty} \tilde{\phi}(k_{\parallel}, x) e^{+ik_{\parallel}z} dk_{\parallel}$$

with each Fourier component governed by the electrostatic dispersion relation

$$\nabla \cdot \vec{\kappa} \cdot \nabla \tilde{\phi} = 0 \quad (2)$$

where $\vec{\kappa}$ is the plasma dielectric tensor. Here, we have neglected coupling to the fast mode and the radiation approximation is taken.

By matching boundary conditions at the interface, we can relate the a_{np} 's and b_{np} 's in terms of plasma and wave parameters. Both these quantities change with plasma loading. However, the limiter plates permit only loose coupling between the antenna and plasma, hence the potential at $x = 0$ normalized by the voltage of the radiating elements (V_p) is essentially unaffected by the plasma loading. As a result, we have

$$a_{np} + b_{np} = A_{np} \quad (3)$$

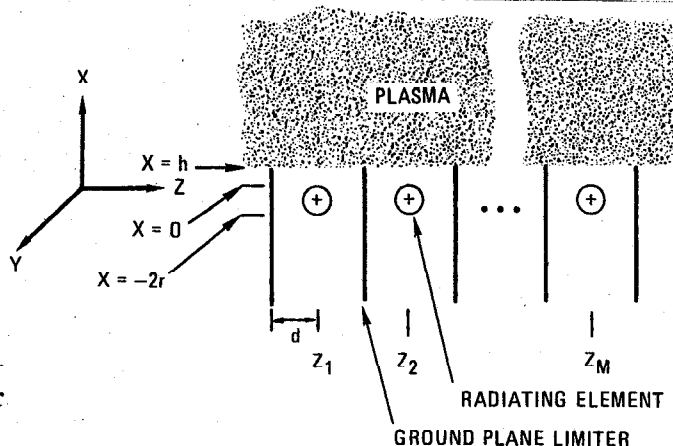


Fig. 1. Idealized version of the slow wave antenna - side view

where the A_{np} 's are the Fourier coefficients of $\phi(o,z)/V_p$ with no plasma loading. They can be evaluated by conformal mapping techniques. The spectrum (in $k_{||}$) is given by

$$P(k_{||}) = \frac{1}{2} \tilde{E}_z(k_{||}, h) \cdot \tilde{E}_z^*(k_{||}, h) \operatorname{Re} Y(k_{||}) \quad (4)$$

$$\text{with } Y(k_{||}) = \frac{-i\omega}{\mu_0 k_{||} c} \frac{\partial \tilde{E}_z}{\partial x}(k_{||}, h) / \tilde{E}_z(k_{||}, h)$$

determined from Eq. (2) and \tilde{E}_z determined from Eq. (1). The total power radiated at the p th element can also be calculated using the Poynting theorem. These quantities are determined in terms of the V_p 's, the voltages at the elements. V_p has to be determined iteratively. Starting with the infinite line approximation (VSWR = 1), the plasma loading is estimated through the power radiated/section. The new voltage along the feedline is then calculated which in turn yields a new plasma loading. The procedure converges in a few iterations. In the next section, this procedure will be applied to analyze the antennas in the experiments.

3. APPLICATION TO EXPERIMENTAL CASE

For our examples, the frequency is fixed at 800 MHz, and the fundamental wavelength $\lambda_{||} = 2.68$ cm ($d = 0.67$ cm), making $n_{||} = 14$. The elements are 0.15 cm in radius and the total structure length is 30 cm. The impedance of the balanced line increases linearly from 100 ohms to 200 ohms along the structure length.

In Fig. 2 we show the plasma loading expressed in terms of the conductance/unit length, G , as a function of the plate height. We note that the loading becomes progressively weaker as h increases, due to the increase in evanescence. Thus the presence of the grounded plates justifies the loose coupling approximation. In subsequent examples as well as in the experiment, h is set equal to 0.2 cm.

Next, we examine the sensitivity of coupling to changes in plasma conditions. In Fig. 3, the loading (in terms of G) is shown as a function of density gradient. Clearly, this case is much less sensitive to the density gradient length than the case when the plates are not present (Fig. 4). That the evanescence imposed by the plates dominates the evanescence due to the plasma is clear.

Finally, the radiated power spectrum, as shown in Fig. 5, is also quite insensitive to changes in density gradient length. Instead of a peak at $n_{||} = \pi c/2\omega d = 14$, there are two peaks at $n_{||} = 14 \pm 1$, which are the consequence of the finite phase velocity along the feedline.

In summary, we have demonstrated by detailed calculations that as a result of the presence of the grounded plates, the antenna coupling is only a weak function of changes in the plasma. The radiated spectrum is well-defined and peaks approximately at the desired wavenumber.

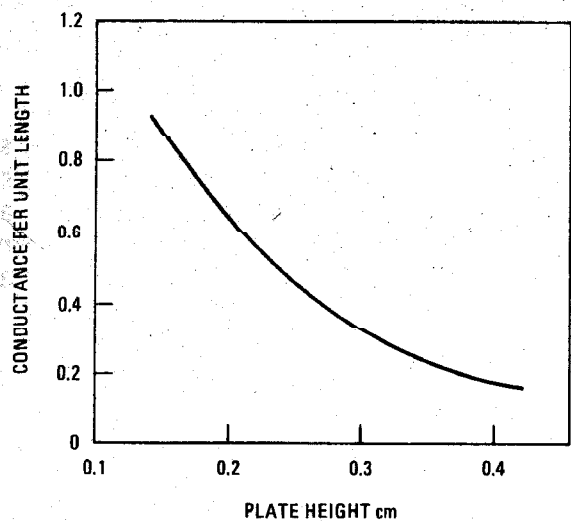


Fig. 2. Calculated plasma loading versus plate height

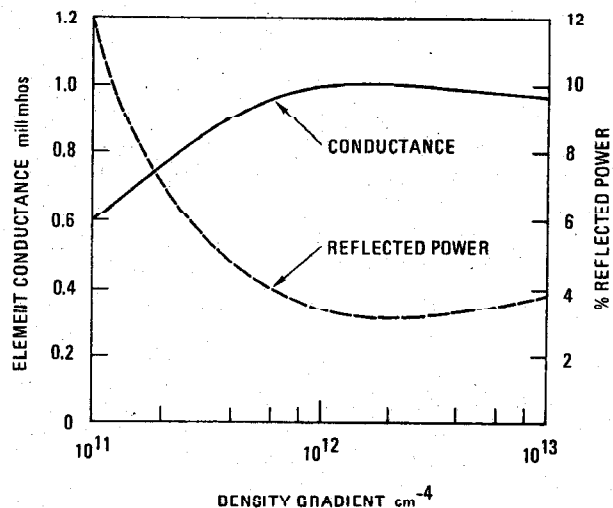
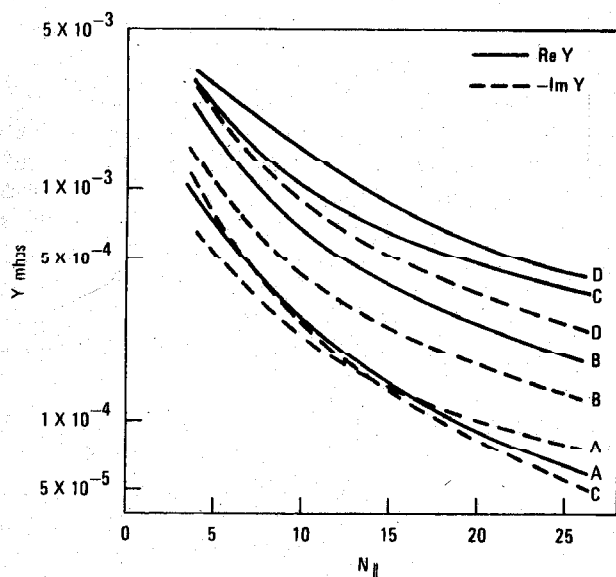


Fig. 3. Calculated plasma loading versus density gradient



A = 10^{11} cm^{-4} ; B = 10^{12} cm^{-4} ;
 C = 10^{12} cm^{-4} with initial density of 10^{11} cm^{-3} ;
 D = 10^{13} cm^{-4}

Fig. 4. Calculated surface admittance of the plasma at the antenna

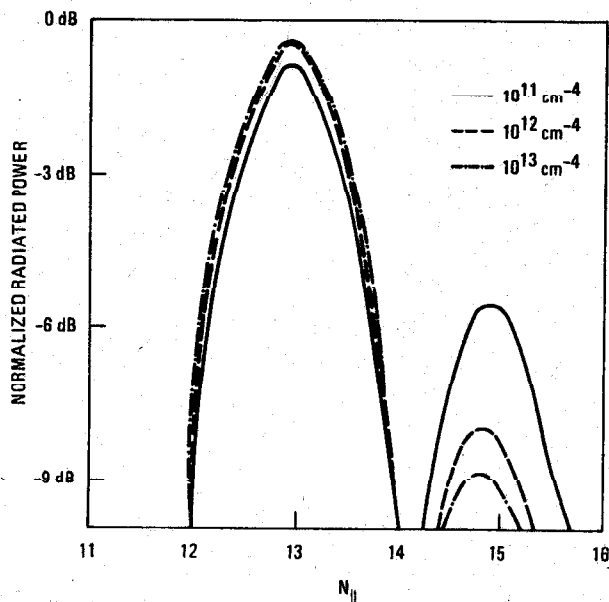


Fig. 5. The calculated radiated spectrum

References

1. M. Porkolab, *et al.*, *Phys. Rev. Lett.* **38**, 230 (1977).
 G. W. Pacher, *et al.*, *Bull. Am. Phys. Soc.* **22**, 1169 (1977), p8F1.
2. V. E. Golant, *Sov. Phys.-Tech. Phys.* **16**, 1980 (1972).
3. V. S. Chan, *et al.*, *Sherwood Theory Meeting*, San Diego, CA 1977, pH2.